Features of soil redistribution and major element migration in a karst hillslope of Southwest China

SONG Chang-shun[1,3] http://orcid.org/0000-0003-2139-7265; e-mail: cssong20061211@163.com

JI Hong-bing[1,2]* http://orcid.org/0000-0003-2438-7716; e-mail: ji.hongbing@hotmail.com

Howard Omar BECKFORD[2] http://orcid.org/0000-0002-9296-3044; e-mail: howbecky@yahoo.com

CHU Hua-shuo[1,3] http://orcid.org/0000-0001-5289-5940; e-mail: chuhuashuo@yahoo.com

ZHANG Kun[1,3] http://orcid.org/0000-0002-5264-7434; e-mail: zhangkun0126@sina.cn

WANG Shi-jie[1] http://orcid.org/0000-0002-6137-1871; e-mail: wangshijie@vip.skleg.cn

* Corresponding author

1 State Key Laboratory of Environmental Geochemistry, Institute of Geochemistry, Chinese Academy of Sciences, Guiyang 550002, China

2 School of Energy and Environmental Engineering, University of Science and Technology Beijing, Beijing 100083, China

3 Graduate University of the Chinese Academy of Sciences, Beijing 100049, China

Citation: Song CS, Ji HB, Beckford HO, et al. (2018) Features of soil redistribution and major element migration in a karst hillslope of Southwest China. Journal of Mountain Science 15(9). https://doi.org/10.1007/s11629-017-4791-3

Abstract: In this study, we investigated the spatial characteristics of the rate of soil distribution and the mechanism of major element migration in a typical karst hillslope in Guangxi Province, Southwestern China. Soil redistribution was examined using ^{137}Cs technique under different hillslope components. With the combination of geochemical methods, the migration characteristics of major elements in soils of three hillslope components in both the horizontal and vertical directions were determined. Thirty-seven soil samples were collected and analyzed for ^{137}Cs and the major elements were determined. By using the profile distribution model the mean soil redistribution rates were found to be -17.01, 0.40 and -23.30 t ha^{-1} yr^{-1} in the summit (BYSD), shoulder (BYSY) and toeslope (BYSJ) components of the studied hillslope, respectively. In comparison to BYSD, the sesquioxides of Fe_2O_3 and TiO_2 tend to be enriched, whereas the alkalis (CaO, MgO, Na_2O and K_2O) tend to be depleted, both in the shoulder and toeslope components. Due to human and animal activities, the contents of CaO, MgO, K_2O and Na_2O have somewhat increased within the topsoil. The results indicated that ^{137}Cs activities are significantly correlated with clay particles and organic matter, and are affected by the pedogenic process and vegatation. Overall, it maybe necessary to use techniques such as ^{137}Cs to investigate soil erosion with the combination of geochemical methods.

Keywords: ^{137}Cs; Karst; Hillslope components; Soil erosion; Major element migration

Introduction

Soil erosion and its associated sedimentation have been considered as one of the major forms of

human-induced soil degradation in karst areas (Parise et al. 2008). Erosion and sedimentation are natural landscape-forming processes, which can be accelerated by human activities through deforestation (Khormali et al. 2009; Ayoubi et al. 2011), overgrazing (Ayoubi et al. 2013) and poor farming practices in different geomorphological hillslope components (Nosrati et al. 2015). This phenomenon causes loss in soil nutrients and land degradation and exacerbates the frequency and intensity of drought, floods, landslides, and other disasters (Rickson 2014; Arnhold et al. 2014). Due to their great impact on environmental conservation and agricultural production, we urgently need to obtain mechanism of the distribution of soil erosion/sedimentation and the migration of soil elements caused by soil redistribution.

In southwestern China, karst areas cover an area of 42.6×104 km², which contains a population of approximately 100 million people (Feng et al. 2016). Soil erosion is one of the most severe environmental problems in southwest China. Many studies have explored a wide range of factors, such as erosion force (Feng et al. 2011), erosion processes (Edgington et al. 1991; Cao et al. 2012), soil degradation (Guo et al. 2015; Feng et al. 2016), and erosion mechanisms (Hancock et al. 2014). However, many studies on soil erosion have focused on non-karst areas (Fernández and Vega 2016), and only a few researches have been conducted in karst areas. Dai et al. (2017) measured both runoff and sediment yield characteristics on the surface and underground of karst bare slopes. They analyzed the impacts of underground pore fissures and bedrock bareness rates on soil erosion; their results showed that rainfall intensity, bedrock bareness rates and the degrees of underground pore fissure are the most important factors affecting soil erosion processes on karst bare slopes. Li et al. (2016b) examined soil erosion in a karst basin using GIS technique and discussed the impact of slope on the temporal and spatial patterns of soil erosion; their results showed that most erosion occurs in areas with slopes of 8°-25°. Bai (2011) calculated recent sedimentation rates in a karst depression; their results showed that between 1963 and 2007 the sediment deposition rates ranged from 0.91 to 1.97 mm yr^{-1}. The existing approach for soil assessment

in karst areas can be generalized into three main categories: erosion measurements in the field (Guo et al. 2015; Dai et al. 2017), integrating remote sensing and geographical information system (GIS)-based investigations (Feng et al. 2016; Huang et al. 2016; Li et al. 2016b), and using radionuclide tracers, such as ^{137}Cs, ^{210}Pb, ^{7}Be and others (Zhang et al. 2009b; Li et al. 2010; Bai 2011; Feng et al. 2016), which can be used to study soil redistribution rates depending on the time-scale involved. The first method, which includes studies of field run-off plots (Dai et al. 2017), may produce accurate measurements of rainfall-induced erosion over a small area; however, obtaining good-quality data requires a great deal of expenditure and fieldwork and cannot be easily applied to a large region. Techniques utilizing the second method, such as the Revised Universal Soil Loss Equation (RUSLE) model (Li et al. 2016b), can generally evaluate the erosion risks in regional landscapes, but they may not be practical in specific environments due to the lack of detailed data that are useful in modeling application (Kheir et al. 2008). Techniques utilizing the third method, such as the ^{137}Cs approach (Bai 2011), offer the potential to quantify soil erosion over large temporal-spatial scales in complex karst landscapes.

^{137}Cs is an artificial radionuclide with a half-life of 30.17 years. ^{137}Cs was released into the atmosphere as the result of nuclear bomb testing and was primarily deposited on the earth's surface due to precipitation during the 1950s-1970s. Regionally, the concentrations of deposited ^{137}Cs vary with rainfall intensity; however, the precipitation is usually uniform within small areas. The deposited ^{137}Cs is strongly and rapidly adsorbed by fine soil particles such as clay minerals and humic materials in the topsoil, and is resistant to chemical or biological removal from soil particles (Zapata 2002; Afshar et al. 2010; Rahimi et al. 2013; Gheysari et al. 2016). ^{137}Cs can provide retrospective estimates of long-term soil erosion (since approximately 1963) and deposition rates over large spatial scales. It can also be used to obtain detailed analyses of sediment migration on hillslopes with different topographic features and land use types (Walling and Quine 1993; Ayoubi et al. 2012a). Previous studies (Li et al. 2009) indicated that it may be problematic to apply the current ^{137}Cs technique to investigate surface

erosion on karst hillslopes in southwest China. This may due to the thin soil cover and the carbonate grains dissolution present in soils. However, well-developed soil exists on the gentle slopes within slight rocky desertification areas or at the edges of karst areas in southwestern China due to the lack of human intervention, perennial vegetation cover, suitable climate, and uniform rainfall. The presence of local land use history and climate condition provided the opportunity to investigate soil erosion using ^{137}Cs technique.

The chemical weathering of rocks supplies mineral nutrients to soils, ground water, rivers and the oceans; it is thus an important component in many biogeochemical systems (Riebe et al. 2003). Due to the serious soil erosion in karst areas, the analysis of the migration of mineral nutrients under soil erosion on different landforms has remained a meaningful research topic. Liu (2009) studied the effects of different landforms on the soil in situ erosion and weathering pedogenesis of karst limestone in southwestern China; their results showed that the topsoil of the foot slope has a lower pH value and lower concentrations of CaO, TiO_2, Al_2O_3, and Fe_2O_3 compared with the top slope. Zhang et al. (2009a) evaluated the soil erosion rates of uncultivated and cultivated land and analyzed the relationship between soil chemical matter (SOC and TN) and soil erosion rates in the Dian Lack catchment in southwestern China. Their results demonstrated that the soil erosion rate is significantly different on different parts of the slope, as it increases from the top to the foot and the middle slope. Additionally, they observed that sites with severe erosion usually have lower SOC and TN contents. Studies in western Iran have revealed that slope gradient significantly influenced the SOC and TN contents, and that steep slopes usually have the lowest values of SOC and TN presumably coincide with accelerated soil erosion (Ayoubi et al. 2012b; Karchegani et al. 2012).

This study investigated a typical karst hillslope in southwestern China. Research on soil erosion and the migration of mineral nutrients has been insufficient in these areas. The specific research objectives of this study were to: (1) measure soil redistribution rate over several spatial and temporal scales on a karst hillslope using ^{137}Cs techniques; (2) assess the impacts of different land use and hillslope components on the variability in ^{137}Cs inventory; and (3) relate soil erosion to the migration of major elements in this area, analyze the main factor influencing the migration of major elements, and discuss the source of soil material in erosion areas.

1　Materials and Methods

1.1 Description of the study area

This study was conducted in Nandan County (24°42′-25°37′N, 107°1′-107°55′E), Guangxi Province, southwest China. This area experienced a warm subtropical monsoon climate. With a mean annual temperature and precipitation of 17.2°C and 1470.2 mm respectively, with almost 65.7% of the rainfall occurs from May to August. The county covers an area of approximately 3916 km² and has an altitudinal range of 500-1000 m above sea level. The main soil type is Brown Rendzina formed from limestone base.

The hillslope studied here is located in Lihu Village (25°07′N, 107°41′E) (Figure 1a). The characteristics of the sampling sites are summarized in Table 1. This hillslope has an altitudinal range of 714.25-764.57 m above sea level, and the distance from the toeslope ranges from 0-175.3 m. The hillslope has a slope gradient of 0°-20° with a parochial road passed at the base. The slope gradient is largest at the toeslope and decreases with elevation; the summit of the hillslope is relatively flat. The hillslope has been covered by
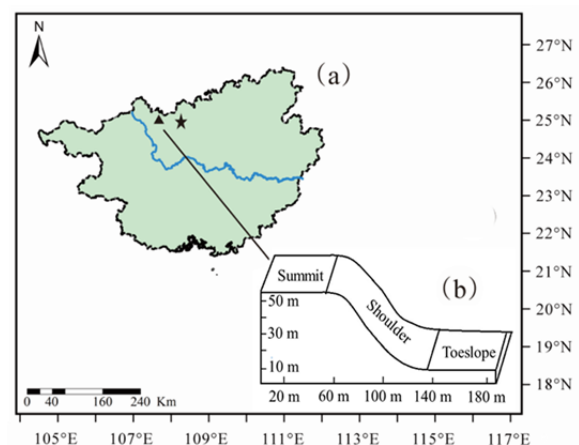
Figure 1 Location of reference (black pentagon) and hillslope sampling sites (black triangle) in Guangxi province, Southwest China (a), and the transection of the studied hillslope (b).

Table 1 The characteristics of the sampling sites in the studied hillslope (BYSD, summit; BYSY, shoulder; BYSJ, toeslope)

Sample	Land use	Hillslope components	Aspect	Elevation (m)	Distance[*] (m)	Gradient (°)
BYSD	G/B	Summit	NW	764.57	175.3	<5
BYSY	F	Shoulder	NW	750.30	105.8	11.85
BYSJ	B	Toeslope	NW	714.25	0[#]	19.93

Notes: G: Grassland; B: Bare land; F: Forestland; NW: Northwestern; [*] the distance from the foot of the hillslope; [#] next to a mountain road, where there is a river across the road.

native forest, following the deforestation of some parts more than 50 years ago due to road construction. No signs of cultivation were found on the hillslope in the last 50 years, although animal excrement was found.

1.2 Soil sampling and measurement

In this study, soil samples were collected in August 2014 from a hillslope containing different land use cover, including forests, grassland and bare land, at its summit (BYSD), shoulder (BYSY) and toeslope (BYSJ) hillslope components, respectively. The transection of the studied hillslopes is illustrated in Figure 1b. Care was taken to ensure that no soil samples were taken from exposed rocks and the concave depositional hollow regions, which were present in each hillslope component. Three even sampling sites were selected, which were located along a water flow line. To save costs and guarantee the accurate measurements of samples, five points in a 9-m² area were selected at each hillslope component. Four of them were located at the vertices of a 3 m×3 m square, and the fifth was located at the center. A scraper plate with an internal soil sampling area of 100 cm^{-2} was used to collect depth-incremental samples (Walling and Quine 1993), using a 2 cm interval from surface to the bedrock approximately more than 30 cm in depth. The same volume of soil was collected at the same interval and was evenly mixed so as to reduce micro-variability. A total of 37 soil samples were collected from the three hillslope components (i.e. summit, shoulder and toeslope) include 13, 11 and 13 soil samples, respectively.

As it was difficult to find completely flat sites with no evidence of soil loss or soil deposit in the study area, an appropriate location for reference sampling was selected in the Huanjiang Observation and Research Station for Karst Ecosystems of the Chinese Academy of Science (CAS), which was located approximately 100 km from the study area (Figure 1a). The reference site was located on a flat area on the top of a hillslope with relatively high soil development characteristics. This site had similar parent material (limestone), aspect (Northwestern) and climate condition (subtropical monsoon climate) as the study site. This reference site had not been affected by severe soil erosion or deposition over the last 50 years and had a permanent grass and shrubs. The annual rainfall values of the study site and reference site are closely comparable (1470.2 mm-1886 mm), and the variation in latitude across these three areas is limited (24°50′N-25°14′N). Three soil profile samples were collected from the reference site at 4 cm depth interval down to the bedrocks (approximately 40 cm).

All samples were air-dried and sieved using a 2-mm mesh sieve and then sent to the Chengdu Institute of Mountain Hazards and Environment, CAS. The ^{137}Cs activity (Bq kg^{-1}) was measured by a gamma spectrometry system using a hyper-pure coaxial germanium detector and a multichannel analyzer. All samples had a weight of 250 g or more. ^{137}Cs activity was detected from 662 keV peak on the spectrum using counting times of greater than 50000 s. The analytical precision was kept at approximately ±5% at the 95% confidence level.

The major element oxide concentrations (SiO_2, Al_2O_3, total Fe as Fe_2O_3, MgO, CaO, Na_2O, K_2O, MnO, TiO_2, P_2O_5, LOI and FeO) of the soil samples were provided by the Beijing Research Institute of Uranium Geology. The soil samples used for the major element analyses were ground to a particle size of 200 mesh using a ball mill and an agate mortar. The element contents of the soil samples were measured using X-ray fluorescence spectrometry (XRF) using a Philips PW2404 X-ray fluorescence spectrometer and referring to the GB/T14506.28-2010 silicate rock chemical analytical procedure.

1.3 Elemental mobility

Depletion and enrichment factors, which indicate the loss or gain of an element in a soil sample in comparison with the parent material, were calculated following the procedures of Nezat et al. (2004).

$$X_{i,j} = (C_{i,j}/C_{i,p})/(Ti_j/Ti_p) \qquad (1)$$

where $C_{i,j}$ and $C_{i,p}$ are the concentrations of element i in soil sample j and the parent material p, respectively, and Ti_j and Ti_p are the concentrations of Ti in soil sample and the parent material, respectively. Although some studies have used Zr, Ti, Nb, or Al as the conservative component (Riebe et al. 2001; Schaller et al. 2009), here, we use Ti as the immobile element because Ti is a major element in common rock-forming minerals and is less likely to suffer from heterogeneity due to its distribution in a trace phase, unlike zirconium. The lowermost soil sample in each sample site was selected to represent the unweathered reference sample.

The enrichment factor can be defined as the loss of an element in samples of rocks, soils and plants (Song et al. 2006):

$$EFX = X_s/X_c - 1 \qquad (2)$$

where X_s and X_c are the concentrations of element X in soil samples and reference samples, respectively. In this study, we used the BYSD samples as reference samples. The values of $EFX =$ 0, $EFX > 0$ and $EFX < 0$ denote the lack of enrichment (or depletion), enrichment or depletion of element X, respectively, in soil samples relative to reference samples.

1.4 Estimation of soil erosion and deposition rates

For uncultivated soils, calculating soil erosion and deposition rates commonly employs a theoretical profile distribution model (Walling and Quine 1990; Zhang et al. 1990; Porto et al. 2001). In most cases, the vertical distribution of ^{137}Cs in uncultivated soils exhibit an exponential decline with depth, described in the following function (Zhang et al. 1990):

$$A'(x) = A_{ref}(1 - e^{-x/h_0}) \qquad (3)$$

where x is the maximum depth of the soil from surface (kg m^{-2}); $A'(x)$ is the concentrations of ^{137}Cs

above the depth x (Bq m^{-2}); and h_0 is the coefficient describing profile shape (kg m^{-2}). The greater the value of h_0, the deeper the ^{137}Cs penetrates into the soil profile.

Assumed that the total fallout of ^{137}Cs occurred in 1963 and that the depth distribution of ^{137}Cs in the soil profile is independent of time, then erosion rate (Y) for an eroding point (total ^{137}Cs inventory of A (Bq m^{-2}) minus the local reference inventory A_{ref} (Bq m^{-2})) can be calculated as follows:

$$Y = \frac{10}{t-1963}\ln(1 - \frac{X}{100})h_0 \qquad (4)$$

where Y is the annual soil loss (t ha^{-1} yr^{-1}) (negative value); t is the year of sample collection (yr); X is the percentage compared with the local ^{137}Cs reference inventory ($\frac{A_{ref}-A}{A_{ref}} \cdot 100$) and A is the measured total ^{137}Cs inventory at the sampling site (Bq m^{-2}).

The model application is simple, and it has been widely used to determine soil erosion rates from ^{137}Cs measurements in areas with undisturbed soils. Only one parameter h_0 needs to be estimated. This measurement can be derived from the vertical distribution of ^{137}Cs in the soil profile at the reference site by fitting the following exponential function to the data:

$$A(x) = A(0)e^{-x/h_0} \qquad (5)$$

where x is the maximum depth from the soil surface (kg m^{-2}), $A(x)$ is the concentration of ^{137}Cs at depth x (Bq kg^{-1}) and $A(0)$ is the concentration of ^{137}Cs in the surface soil (Bq kg^{-1}).

Using the Laniarius least squares regression, Eq. (3) was fitted to the vertical distribution of ^{137}Cs activity (Bq kg^{-1}) for the reference site. Then the parameters value $A(0)$ and h_0 were determined.

2 Results

2.1 Reference site

Zhang et al. (2017) reported a ^{137}Cs reference inventory as 891.6 Bq m^{-2} measured in 2009 for this reference site. Li et al. (2010) calculated another reference inventory as 998 Bq m^{-2} measured in 2006 in Luoyang Town which is about 6 km away from the reference site. These two reference inventories for 2014 were 793.68 and 828.49 Bq m^{-2} corrected for radioactive decay, respectively. Considering the short distance

between these reference sites, we used all five reference inventories for calculating the mean reference inventory. The coefficient of variation (*CV*) of total ^{137}Cs inventory for five sites was 7.67% with mean value of 883.86 Bq m^{-2} and variance of 5740.23. Minimum number of reference samples with less than 10% error at the 95% confidence level and coefficient of variance of 10% is four (Pennock et al. 2007). In this study, the minimum number of reference samples needed to obtain the mean reference inventory with less than 10% error at the 95% confidence level is one, which was estimated using the Survey Software developed by The Creative Systems (2016).

The maximum depth of ^{137}Cs penetration ranged from 32-36 cm in the first reference core (Figure 2). A large quantity of ^{137}Cs activity (~80%) was concentrated in the upper 12 cm of this site and the profile demonstrated near-exponential decline in ^{137}Cs activity with depth (Collins et al. 2001). The ^{137}Cs inventories of the five other sites were similar. The ^{137}Cs reference inventory measured in 2009 in the Yaji experimental site in Guilin City, which was located approximately 250 km from the study area, was 1038.4 Bq m^{-2} (Li et al. 2016a), and the reference inventory measured in 2014 was 924 Bq m^{-2} when corrected for radioactive decay. It is well-known that the deposition flux of ^{137}Cs from the atmosphere is predominantly controlled by precipitation, latitude, and local climate (Shi et al. 2012). All of the sites located in northern Guangxi Province are characterized by a subtropical monsoon climate. The annual rainfall values of these three areas are closely comparable (1470.2 mm-1886 mm), and the variation in latitude across these three areas is
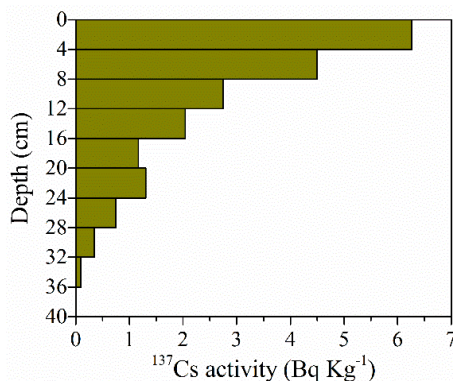
Figure 2 Vertical distribution of ^{137}Cs inventory in the reference site, core NO. 1, in the selected reference site in southwest China.

limited (24°50′N-25°14′N). Hence, it appeared to be reasonable to use a reference value of 883.86 Bq m^{-2} for this study area.

2.2 137Cs records

Figure 3a, b, c show the vertical distribution of ^{137}Cs activity in BYSD, BYSY and BYSJ profiles located in the summit, shoulder and toeslope, respectively of the studied hillslope. Figure 3a shows that the ^{137}Cs concentration tends to be evenly distributed within the upper 6 cm. Under the peak in activity concentration at a depth of 4-6 cm (2.95 Bq kg^{-1}), the profile shows an exponential decrease in ^{137}Cs activity with depth, which drops to 0.06 Bq kg^{-1} at a depth of 14 cm. The depth distribution profile of ^{137}Cs in Figure 3b is similar to the profile shown in Figure 3a. The ^{137}Cs concentration peak is located at a depth of 0-2 cm. The ^{137}Cs concentration tends to be evenly distributed within the upper 8 cm; it then decreases exponentially with increasing depth and drops to 0.69 Bq kg^{-1} at a depth of 16 cm. Figure 3c shows an obviously exponential decrease in ^{137}Cs activity with depth. Below the ^{137}Cs concentration peak at the surface layer of 0-2 cm (3.63 Bq kg^{-1}), it decreases exponentially with depth and drops to 0.19 Bq kg^{-1} at a depth of 16 cm.

2.3 Major element analysis

The major element contents of these samples are listed in Table 2, as are the corresponding mean values of major elements in the upper continental crust (UCC) (Taylor and Mclennan 1985). These data showed that the most abundant compounds found within the soil samples in the three components (BYSD, BYSY and BYSJ) are SiO_2, Al_2O_3 and Fe_2O_3, with the mean values of 85.2, 85.7 and 87.3 weight percentage (wt.%), respectively. The contents of MnO, P_2O_5 and Na_2O in the three profiles are within the ranges of 0.031%-0.157%, 0.06%-0.121% and 0.032%-0.132%, respectively, which are close to their detection limits. The profiles have the similar average concentrations of K_2O, CaO and MgO, which are within the ranges of 0.22%-0.51%, 0.30%-0.41% and 0.21%-0.49%, respectively. The mean LOI for the BYSD, BYSY and BYSJ profiles were found to be 10.92%, 10.65% and 9.42%,
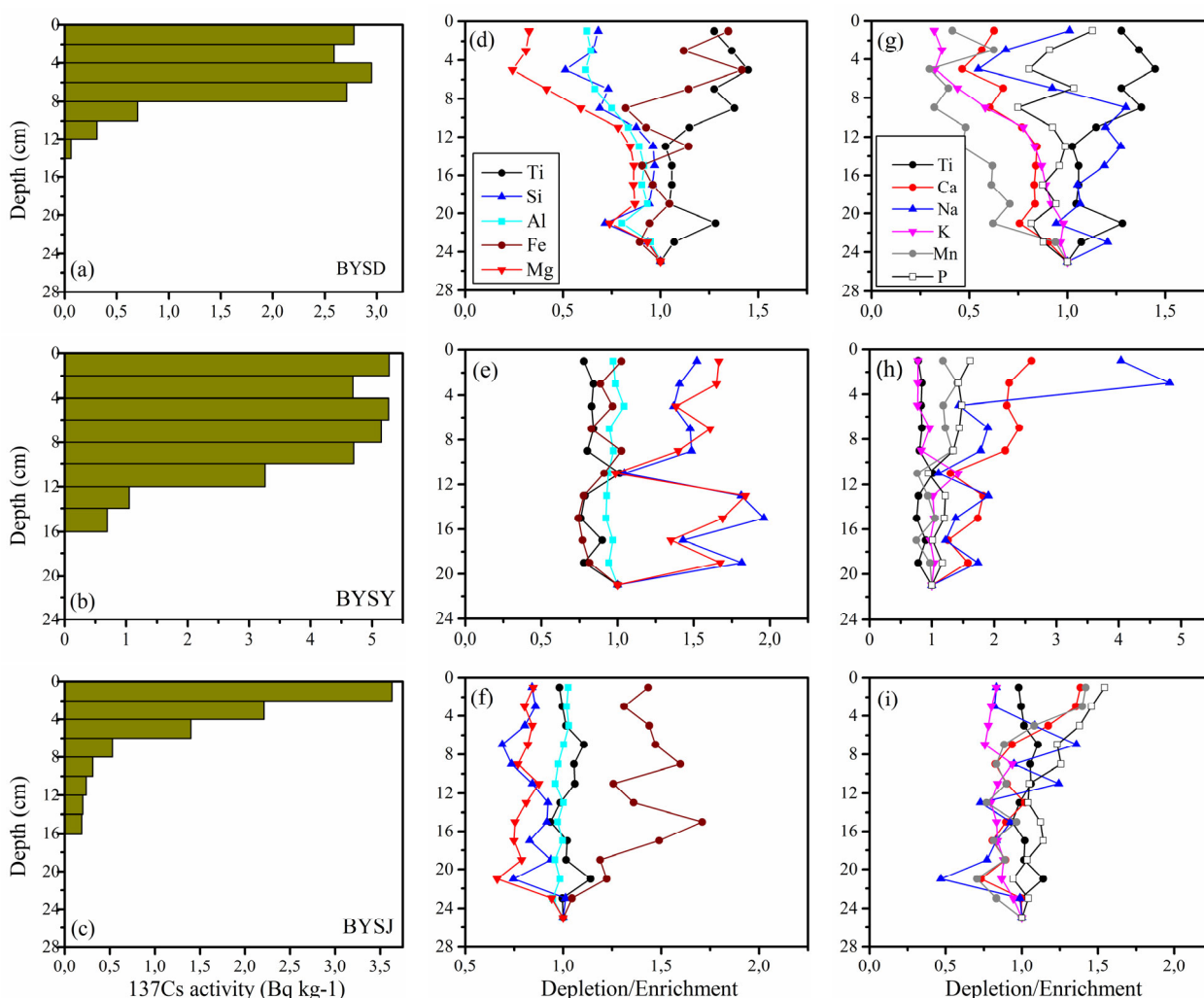
Figure 3 Depth distribution profiles of ^{137}Cs activity and depletion/enrichment factors. (a), (d) and (g) the depth distribution of ^{137}Cs activity and depletion/enrichment factors in the BYSD (summit) profile; (b), ((e) and (h) the depth distribution of 137Cs activity and depletion/enrichment factors in the BYSY (shoulder) profile; (c), (f) and (i) the depth distribution of 137Cs activity and depletion/enrichment factors in the BYSJ (toeslope) profile.

respectively and the CIA values were also found to be 0.954%, 0.969% and 0.969% respectively in this studied hillslope.

Because these three groups of soil samples have statistically similar major element compositions, as is demonstrated above, the 37 soil samples collected from these three sampling sites are grouped into one. Descriptive statistics (n = 37) show that MnO, MgO and K_2O have the highest CV (coefficient of variation) values, whereas TiO_2, Al_2O_3 and SiO_2 have the lowest CVs. For individual groups of samples, MgO has the highest CV (31.45%) and Al_2O_3 has lowest CV (7.84%) in the BYSD soil samples (n = 13); Na_2O has the highest CV (58.52%) and TiO_2 has the lowest CV (10.39%) in the BYSY soil samples (n = 11); and Na_2O has the

highest CV (26.87%) and TiO_2 has the lowest CV (5.36%) in the BYSJ soil samples (n = 13). The relatively low values of the CVs of the major elements in these three groups suggest that these major element compositions are relatively consistent within these three groups of samples, and the major element with the highest CV in each group indicates that the content of this major element mostly varies with depth within each sampling profile.

3   Discussion

3.1 Soil redistribution assessment of the studied hillslope

Table 2 The depth distribution of major oxides, with average values of these oxides and those of the upper continental crust (UCC)

Sample No	Depth (cm)[a]	Major elements (wt%)[c]										LOI[d]	FeO	CIA[e]
		SiO2	Al2O3	Fe2O3[b]	MgO	CaO	Na2O	K2O	MnO	TiO2	P2O5			
BYSD-1	1+2	46.15	13.91	25.05	0.265	0.376	0.08	0.257	0.082	1.99	0.095	11.50	1.96	0.963
BYSD-2	3+2	47.30	15.37	22.29	0.269	0.362	0.058	0.31	0.133	2.13	0.082	11.43	2.15	0.967
BYSD-3	5+2	39.51	15.63	29.91	0.224	0.316	0.049	0.296	0.067	2.26	0.077	11.39	1.34	0.970
BYSD-4	7+2	49.65	14.82	21.26	0.337	0.404	0.073	0.353	0.078	1.99	0.087	10.56	1.58	0.960
BYSD-5	9+2	50.43	18.13	16.50	0.518	0.392	0.111	0.504	0.069	2.15	0.068	10.87	0.99	0.952
BYSD-6	11+2	53.45	16.77	15.50	0.57	0.415	0.085	0.56	0.086	1.79	0.07	10.67	1.08	0.950
BYSD-7	13+2	52.44	16.02	17.11	0.55	0.408	0.081	0.539	0.074	1.6	0.067	10.84	1.07	0.950
BYSD-8	15+2	54.49	16.98	13.97	0.58	0.418	0.078	0.579	0.102	1.65	0.067	10.77	1.24	0.951
BYSD-9	17+2	53.93	16.77	14.82	0.579	0.414	0.069	0.593	0.101	1.65	0.061	10.58	0.82	0.951
BYSD-10	19+2	52.34	17.09	15.94	0.577	0.411	0.069	0.604	0.115	1.63	0.065	10.84	0.85	0.951
BYSD-11	21+2	48.81	18.00	17.64	0.602	0.457	0.075	0.792	0.124	2	0.069	10.69	0.81	0.942
BYSD-12	23+2	53.27	17.80	13.95	0.634	0.455	0.08	0.651	0.157	1.67	0.062	10.91	1.48	0.948
BYSD-13	25+2	53.13	17.52	14.58	0.635	0.471	0.062	0.63	0.156	1.56	0.066	10.92	0.73	0.952
Mean value		50.377	16.524	18.348	0.488	0.408	0.075	0.513	0.103	1.852	0.072	10.92	1.24	0.954
BYSY-1	1+2	48.51	14.44	20.65	0.218	0.488	0.132	0.18	0.045	2.15	0.083	13.00	2.73	0.958
BYSY-2	3+2	48.44	15.82	19.28	0.233	0.454	0.17	0.194	0.058	2.32	0.079	12.86	2.29	0.954
BYSY-3	5+2	46.51	16.51	20.75	0.193	0.44	0.05	0.191	0.048	2.29	0.081	12.82	1.58	0.978
BYSY-4	7+2	50.87	15.19	17.99	0.227	0.487	0.067	0.242	0.05	2.32	0.08	12.24	1.95	0.969
BYSY-5	9+2	48.74	14.86	21.22	0.188	0.42	0.06	0.199	0.052	2.21	0.071	11.79	1.57	0.973
BYSY-6	11+2	43.41	18.2	23.94	0.168	0.317	0.047	0.43	0.038	2.8	0.063	10.51	0.67	0.967
BYSY-7	13+2	58.34	13.94	15.82	0.243	0.345	0.063	0.238	0.036	2.17	0.063	8.36	1.01	0.968
BYSY-8	15+2	60.82	13.34	14.53	0.215	0.317	0.044	0.234	0.039	2.09	0.06	7.93	1.13	0.971
BYSY-9	17+2	52.6	16.61	17.89	0.204	0.273	0.046	0.261	0.033	2.48	0.06	9.27	0.61	0.975
BYSY-10	19+2	57.91	14.02	16.43	0.219	0.296	0.057	0.241	0.037	2.15	0.06	8.14	0.96	0.969
BYSY-11	21+2	40.96	19.09	25.88	0.168	0.241	0.042	0.298	0.049	2.76	0.066	10.18	0.76	0.976
Mean value		50.646	15.638	19.489	0.207	0.371	0.071	0.246	0.044	2.340	0.070	10.65	1.39	0.969
BYSJ-1	1+2	48.87	13.33	22.61	0.211	0.399	0.049	0.205	0.057	1.96	0.121	11.84	1.81	0.972
BYSJ-2	3+2	50.64	13.42	20.99	0.203	0.396	0.049	0.2	0.057	1.99	0.116	11.66	1.45	0.973
BYSJ-3	5+2	48.38	13.84	23.5	0.217	0.35	0.066	0.199	0.045	2.03	0.112	11.05	1.35	0.970
BYSJ-4	7+2	45.13	14.69	26.15	0.23	0.304	0.09	0.21	0.04	2.21	0.109	10.72	1.21	0.966
BYSJ-5	9+2	46.08	13.62	27.14	0.206	0.256	0.06	0.248	0.036	2.11	0.106	9.95	0.92	0.967
BYSJ-6	11+2	52.88	13.47	21.42	0.236	0.281	0.079	0.224	0.039	2.12	0.089	8.90	0.86	0.964
BYSJ-7	13+2	53.85	13.07	21.54	0.203	0.295	0.043	0.197	0.031	1.97	0.082	8.43	1.06	0.974
BYSJ-8	15+2	50.78	12.04	25.73	0.179	0.246	0.052	0.196	0.037	1.87	0.084	8.45	0.61	0.969
BYSJ-9	17+2	50.07	13.48	24.46	0.194	0.242	0.051	0.215	0.034	2.04	0.093	8.84	0.85	0.971
BYSJ-10	19+2	56.4	12.89	19.41	0.203	0.266	0.047	0.224	0.037	2.03	0.084	8.06	0.92	0.970
BYSJ-11	21+2	50.42	14.86	22.41	0.192	0.245	0.032	0.248	0.033	2.28	0.086	8.83	0.98	0.975
BYSJ-12	23+2	59.7	12.49	16.71	0.238	0.291	0.059	0.236	0.034	1.99	0.083	7.79	0.86	0.965
BYSJ-13	25+2	59.28	13.26	16.09	0.254	0.294	0.06	0.251	0.041	2	0.08	7.96	1.18	0.966
Mean value		51.729	13.420	22.166	0.213	0.297	0.0567	0.219	0.040	2.046	0.096	9.42	1.08	0.969
UCC[f]		66.000	15.200	5.000	2.200	4.200	3.900	3.400	0.080	0.500	0.160			

Notes: [a] The sampling depth + sampling interval (2 cm); [b] Total iron, expressed as Fe2O3; [c] All the major element values are in weight percent; [d] Loss on ignition (LOI); [e] Chemical index of alteration (CIA) = Al2O3/(Al2O3+CaO*+Na2O+K2O), where CaO* only represents the Ca in silicate (Nesbitt and Wilson 1992); [f] The mean chemical composition of the Upper Continental Crust (UCC).

The ^{137}Cs inventories and soil redistribution of different hillslope components are shown in Table 3. The ^{137}Cs inventories were 363.0, 902.7, and 261.3 Bq m^{-2} at the summit, shoulder and toeslope, respectively. As is shown in Figure 4, except for the ^{137}Cs inventory at the shoulder, the other two ^{137}Cs inventories were less than the local reference inventory (889.8 Bq m^{-2}). This indicates that soil erosion occurred at the summit and toeslope of the hillslope, whereas soil deposition only occurred at the shoulder. According to the profile distribution model (Zhang et al. 1990), the annual redistribution rates were -17.01, 0.40, and -23.30 t ha^{-1} yr^{-1} at the summit, shoulder and toeslope of the studied hillslope, respectively. These results are contrary to other scholars, which indicated that the highest degree of soil erosion occurred at the shoulder and the lowest degree of erosion occurred at the toeslope (Afshar et al. 2010; Ayoubi et al. 2012a; Rahimi et al. 2013). We suggest that this apparent discrepancy is caused by terrain factors and the effects of human activities. Afshar et al. (2010) reported that significantly positive correlations were detected between ^{137}Cs inventories and some topographic attributes such as slope, sediment transport index and specific catchment area. Rahimi et al. (2013) has reported the highest erosion rates of 3.94 - 90.1 and 86.41 - 159.3 t ha^{-1} yr^{-1} in the shoulder components of the natural pasture and the cultivated soils, respectively. While these phenomena always appeared in single-factor cases, the results could be different in this studied hillslope due to the different land use type and slope in each hillslope component.

Our observations are similar to those obtained by Popa et al. (2011). Popa et al. (2011) reported that soil deposition occurred at the middle hillslope position inside forest belts, while most of the sampling sites outside forest belts had lower ^{137}Cs inventories than the reference inventory. On the shoulder of the hillslope, the surface runoff from the summit of the hillslope has a lower velocity and flux due to the obstructions of the forest root system and litter fall. Ayoubi et al. (2012a) reported that the soil erosion occurred in the summit position and that soil cultivation and tillage practices are the major factors affecting soil loss from the summit position. By visiting aborigines and field surveys, we confirmed that the

Table 3 The ^{137}Cs inventories and soil redistribution at different hillslope components (BYSD, summit; BYSY, shoulder; BYSJ, toeslope)

Sample	Hillslope components	^{137}Cs Inventory (Bq m^{-2})	Soil redistribution (t ha^{-1} yr^{-1})
BYSD	Summit	363.0	-17.01
BYSY	Shoulder	902.7	0.40
BYSJ	Toeslope	261.3	-23.30
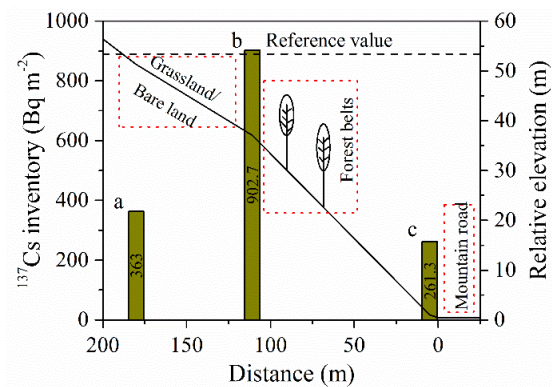
Figure 4 ^{137}Cs inventories of the three soil profiles and the characteristics of these sampling sites. (a) BYSD (summit) profile; (b) BYSY (shoulder) profile; (c) BYSJ (toeslope) profile.

hillslope has not been cultivated since the initial isotope fallout. The observed soil erosion in the summit position of this studied hillslope could be attribution to surface soil erosion induced by low vegetative coverage and animal activities, which may be supported by the presence of animal excrement on the hillslope. On the toeslope of the hillslope, there is no vegetative cover that can protect the soil against erosion; this site also has the greatest slope gradient, especially because a mountain road exists at the foot of the hillslope, with a river located on the opposite side. It is thus reasonable to assume that eroded material from higher components will be carried away to the river by runoff. These results indicate that the ^{137}Cs activity and inventory, as well as erosion/deposition, were significantly affected by terrain factors (i.e., slope and hillslope components) and the interference of human activities (i.e., deforestation and the construction of roads). In other words, the human interference such as road constructions and deforestation, can accelerate soil erosion, which is confirmed in the BYSY (shoulder) and BYSJ (toeslope) sites.

The soil formation rates in karst areas in southwestern China have been estimated to range

from 0.04 to 1.2 t ha^{-1} yr^{-1} (Li et al. 2006; Cao et al. 2008). According to our measurements, the mean annual soil erosion rates of the summit and toeslope components in this hillslope are 20 times higher than the soil formation rates. This implies that a large proportion of sediments may have reached the river system. The high erosion rates at the summit and toeslope components must have been due to the combined effects of runoff and deforestation. Soil erosion hazards in this study area should not be ignored. Man-made measures of natural vegetation protection and the assessment of the environmental impact of road construction are suggested to be the first important approaches to reduce soil erosion on karst hillslopes in this study area.

3.2 The characteristics of major element migration

3.2.1 The inheritance of erosion materials

Compared with the mean chemical composition of the Upper Continental Crust (UCC) (Figure 5), the distribution patterns of major elements in the soils of the BYSD, BYSY and BYSJ sampling sites are, overall, quite similar. The BYSD samples are enriched in MgO, K$_2$O and MnO compared with the BYSY and BYSJ samples. The BYSJ samples are slightly depleted in CaO and Na$_2$O relative to the BYSJ samples. The SiO$_2$, MgO, CaO, Na$_2$O, K$_2$O and P$_2$O$_5$ contents of all samples are lower than those of the UCC, and the Fe$_2$O$_3$ and TiO$_2$ contents of all samples are higher than those of the UCC. The remarkable enrichments of Ti and Fe in all three soil profiles reflect the existence of Ti-bearing minerals, such as ilmenite, rutile and titanite, and Fe-oxides, such as magnetite, hematite and goethite, respectively. The MnO content of the BYSD samples is higher than that of the UCC, while the MnO contents of the BYSY and BYSJ samples are lower than that of the UCC. Overall, the distribution patterns of the major elements in the BYSY and BYSJ samples are more similar to each other due to the accumulation of erosion materials from the summit of the hillslope. In contrast, the soil of the BYSD site is provided by the weathering of overlying carbonate rocks; thus, relative to the BYSY and BYSJ samples, the distribution patterns of major elements in the BYSD samples are closer to the UCC curve. These observations indicate that

the soils of the three profiles have a good affinity to each other.
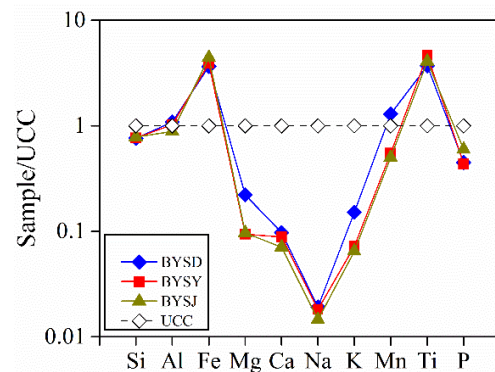
Figure 5 The distribution patterns of major elements in the three soil profiles (BYSD, summit; BYSY, shoulder; BYSJ, toeslope) compared with the mean chemical composition of the Upper Continental Crust (UCC).

Al and Ti are the least mobile elements during chemical weathering, TiO$_2$/Al$_2$O$_3$ ratios have been used as a provenance indicator (Young and Nesbitt 1998). There is a positive correlation (R^2 = 0.607) between TiO$_2$ and Al$_2$O$_3$ in all samples (Figure 6a) of the three soil profiles, thus reflecting that they may have a cognate relationship. The positive correlation (R^2 = 0.980) between TiO$_2$ and Al$_2$O$_3$ in the BYSY and BYSJ samples (Figure 6b) is more significant than that in three profile samples, which is probably due to the migration of Al as a result of chemical dissolution or the physical migration of an Al-rich phase (e.g., clay minerals) with soil erosion (Maynard 1992; Young and Nesbitt 1998). There is a significant correlation between the upper four soil samples of the BYSD profile and the BYSY and BYSJ soil samples (R^2 = 0.963) (Figure 6c). Muhs et al. (2013) assessed whether Fe in that size fraction is potentially bioavailable in seawater and proposed that dust with a relatively high bulk Fe content may yield little soluble Fe to the marine environment if most of the Fe-bearing minerals are in the form of Fe oxides. There is a positive correlation (R^2 = 0.632) between Fe$_2$O$_3$ and TiO$_2$ in all samples (Figure 6d) in this study, which may be due to the fact that Fe (III) is the dominant cation. We recognize that unlike most immobile elements (e.g., Ti and Al), K and Mg are potentially mobile in near-surface soil zones (Muhs et al. 2010). Lanzarote Island, the study area of Muhs, has a mean annual precipitation of only 100-200 mm yr^{-1} and a substrate that is only *c.* 21 ka old; thus, these

soils have probably experienced minimal chemical weathering. Almost all samples show a significant correlation between K_2O and MgO (Figure 6e), suggesting the intense and synchronous chemical weathering of K-bea ring minerals (e.g., K-feldspar and illite) and Mg-bearing minerals (e.g., calcite and dolomite). The correlation rate between SiO_2 and Fe_2O_3 is 0.592 (Figure 6f), which may be a result of fine mineral inclusions and/or the precipitation of SiO_2 on the surfaces of Fe-bearing minerals (Bischoff 1969; Taitel-Goldman et al. 2004). It is obvious that the lower samples (dashed area in Figure 6a, d, e, f) in the BYSD profile show weaker chemical weathering relative to the upper four samples; this may be due to intense soil erosion creating a thin layer of highly weathered soil.

Combined with the erosion characteristics of this hillslope discussed above, these results show that the soils from these three profiles may have been derived from an identical material. They also demonstrate that the BYSY (shoulder) and BYSJ (toeslope) profiles record the inheritance of erosion material from the BYSD (summit) profile.

3.2.2 Lateral migration of major elements

To show the lateral migration of major elements along the hillslope under the action of soil erosion and deposition, we calculated the elemental enrichment factors of the BYSY (shoulder) and BYSJ (toeslope) samples relative to the BYSD (summit) samples (Figure 7). Figure 7
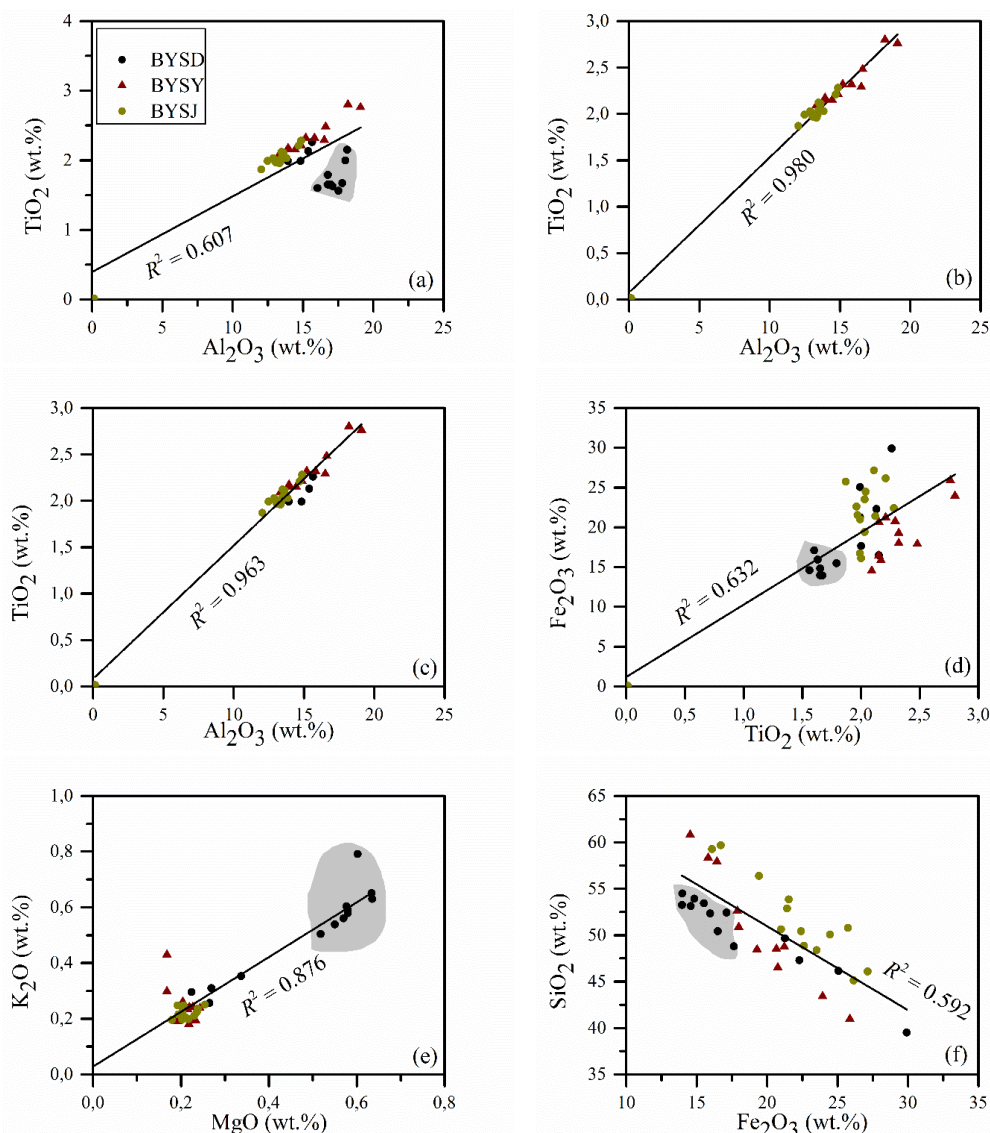

Figure 6 Relationships between Al_2O_3 and TiO_2, K_2O and MgO, Fe_2O_3 and TiO_2, SiO_2 and Fe_2O_3 in three soil profiles.

reflects, to some extent, the migration characteristics of major elements from the summit of the hillslope to the toeslope of the hillslope. The contents of MnO, MgO, K_2O, CaO, Na_2O and Al_2O_3 in the BYSY and BYSJ samples are significantly depleted relative to those in the BYSD samples. These elements, except for Al, are highly soluble in soil solutions and can be exported along the hillslope by rainfall; thus, they are unlikely to be enriched on the shoulder and toeslope of the hillslope. Because Al is less mobile, it should be enriched in the BYSY and BYSJ samples; however, it is likely depleted in the BYSY and BYSJ samples due to organic matter, especially organic acid, playing a role in transporting Al. Land and Öhlander (2000) observed very high dissolved concentrations of Al in the E-horizon of a soil profile with a low pH value and high concentrations of complexing organic acids. TiO_2 and Fe_2O_3 (in which, as discussed above, Fe(III) may be the dominant cation) are enriched in the BYSY and BYSJ samples because they are less mobile and can be enriched in depositional areas where soil erosion occurred at the summit of the hillslope. P_2O_5 and SiO_2 are enriched in the BYSJ samples, and they are neither enriched nor depleted in the BYSY samples, although soil deposition occurred at the BYSY site and soil erosion occurred at the BYSJ site. These results indicate that the major elements of Fe and Ti tend to be enriched in the lower part of the hillslope relative to the summit of the hillslope due to physical migration, although soil erosion occurred at the toeslope of the hillslope; Mn, Mg, K, Ca, Na and Al tend to be depleted in the lower parts of the hillslope relative to the summit of the hillslope due to soil erosion; P and Si show no obvious trends of enrichment or depletion on the hillslope components.

3.2.3 Vertical distribution of major elements

In order to assess the enrichment mechanisms of major elements in soil samples, the depletion and enrichment factors were calculated (Taylor and Blum 1995; Nezat et al. 2004). The depth distributions of the depletion and enrichment factors based on the major element concentrations in the three depth profiles are shown in Figure 3d-i. In the BYSD depth profile (Figure 3d and g), SiO_2,
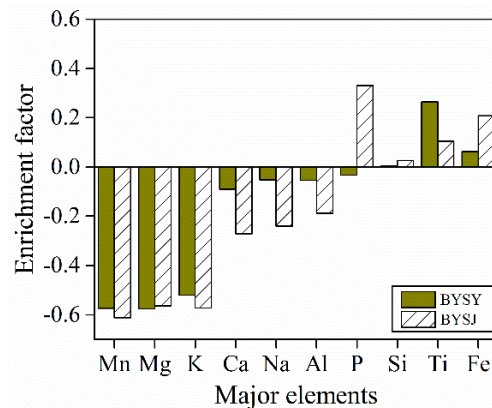
Figure 7 The elemental enrichment factors of the BYSY (shoulder) and BYSJ (toeslope) profiles relative to the BYSD (summit) profile.

Al_2O_3 and CaO show depletion factors ranging from 0.5-0.9, and Fe_2O_3, Na_2O and P_2O_5 are neither enriched nor depleted. MgO, MnO and K_2O are depleted to values as low as 0.3. TiO_2 is most enriched (1.45) at a depth of 4-6 cm, while the highest value of ^{137}Cs is observed at the same depth. As mentioned earlier, ^{137}Cs is strongly adsorbed to fine particles in the surface soil, especially clay minerals and humic materials (Zapata 2002). TiO_2 might migrate to this depth combined with humic materials. This indicates that a large amount of humic materials may exist at this depth in the profile. Na_2O, K_2O, CaO, MgO, MnO and SiO_2 are most depleted at a depth of 4-6 cm because these elements are highly soluble and can be preferentially exported from the soil profile in soil solution (Ji et al. 2004). This phenomenon indicates that a large amount of soil water may exist at this depth in the soil profile. In the BYSY depth profile (Figure 3e and h), TiO_2, Fe_2O_3 and Al_2O_3 are neither enriched nor depleted because these elements are less mobile and tend to be concentrated in typical weathering products, such as clay minerals and oxides. Yousefifard et al. (2012) stated that immobile element are redistributed within weathered profile and can be leached out of the weathering profiles under certain conditions. MnO, K_2O and P_2O_5 are also neither enriched nor depleted, and the changes in the depletion and enrichment factors of these mobile elements with depth indicate that supplements of these elements exist that can counteract their removal by leaching. SiO_2, MgO, CaO and Na_2O show enrichment factors between 1 and 4.8, and Na_2O is most enriched (4.8) at a depth

of 2-4 cm. These results also indicate that supplements of these mobile elements exist due to the soil erosion of the BYSD site and the soil deposition of this site. In the BYSJ depth profile (Figure 3f and i), TiO_2 and Al_2O_3 are neither enriched nor depleted. MgO, SiO_2, and K_2O show depletion factors ranging from 0.6-0.9. Fe_2O_3 shows enrichment factors ranging from 1-1.7. MnO, P_2O_5 and CaO are enriched in the upper soil profile (0-6 cm) and depleted in the lower part of the soil profile. Na_2O shows no clear tendency; this may be because soil erosion occurs at this site, whereas soil deposition occurs due to the site location i.e toeslope of the hillslope.

These results show that the depletion and enrichment factors of major elements in different hillslope components varied significantly, perhaps due to the impacts of topography and leaching. The depletion and enrichment factors of most major elements in the BYSY profile are higher than those in the BYSD and BYSJ profiles, which probably indicates that the intensity of the chemical weathering of the BYSY profile is higher than those of the BYSD and BYSJ profiles. Less mobile elements, such as Al, Ti and Fe, exhibit no obvious differences in their depletion and enrichment factors in three soil profiles, while Al is depleted in the BYSD profile (Figure 3d) (Hill et al. 2000; Kurtz et al. 2000). Under supergene conditions, Ti was deposited in slope sediments in the form of titanium hydroxide ($TiO_2 \cdot nH_2O$) during the weathering of titanium minerals; then, part of this compound lost its water and was recrystallized. Therefore, during crustal weathering, relative increases in titanium are due to decreases in the contents of mobile elements (Mou 1999). The solubility of iron is controlled by oxidation-reduction conditions; reduction conditions and an acidic medium favor the transport of iron, whereas iron is easily decomposed under oxidation conditions and in an alkaline medium. Schroth et al. (2009) obtained consistent results when they confirmed that minerals in which Fe is in its ferrous, or Fe(II) form, yield much more Fe in leaching experiments than minerals in which Fe is in its ferric, or Fe(III), form. This may explain the enrichment of Fe_2O_3 in the BYSJ profile (Figure 3f). Al is an important soil element, and its ionic charge does not change; therefore, the migration and transformation of Al during crustal weathering is not directly affected by oxidation-reduction conditions. Generally, it is hard to dissolve Al in water, and it is hard for Al to migrate downwards in solution (Nesbitt and Wilson 1992). However, the migration of Al is mainly affected by the degradation of organic matter in subtropical climates, and the degradation of organic matter is affected by oxidation-reduction conditions (Viers et al. 2000; Braun et al. 2005). Under oxidation conditions, many organic colloids continue to break down, leading to the decreased adsorption capacity of Al and resulting in the accumulation of Al. Perhaps due to human and animal activities, the contents of CaO, MgO, K_2O and Na_2O somewhat increased within the topsoil; a similar observation was made by Feng et al. (2009). The temporal and spatial variations in the dissolved Si in soil water resemble those of Na, Ca, Mg and Sr, and Mn appears to be more mobile further down in the soil compared with Fe and Al (Land and Öhlander 2000). These results are consistent with the observations made in this study (Figure 3d-i). In mid-latitude soils, total P typically exhibits enrichment at the surface (due to biocycling), depletion just below this zone (due to both leaching and plant uptake), and relatively high values below the zone of depletion, where neither leaching nor the plant uptake of P are active processes (Runge et al. 1974). This "high-low-high" depth function also appeared in this study (Figure 3d-i).

3.3 Relationships between ^{137}Cs and major element

Recent studies have investigated the correlation between soil physico-chemical parameters and ^{137}Cs in different regions including cultivated and uncultivated fields. For example, Rahimi et al. (2013) reported statistically significant positive correlations between ^{137}Cs inventory and mass magnetic susceptibility in both pasture and cultivated lands. Nosrati et al. (2015) found statistically significant positive correlations between ^{137}Cs inventory and soil organic carbon tock in both cultivated and forest soils.

There was a positive correlation (R^2 = 0.836) between ^{137}Cs activities and the chemical index of alteration (CIA) in the BYSD (summit) soil samples (Figure 8a). The CIA predominantly tracks feldspar dissolution and the concomitant release of Ca, Na,

and K relative to Al, since the latter is typically retained within pedogenetic clays (Babechuk et al. 2014). This result indicates that ¹³⁷Cs is strongly and quickly adsorbed to clay particles within the soil. There was no significant correlation between ¹³⁷Cs activities and CIA values in lower positions (BYSY and BYSJ), this may be as a result of the BYSY and BYSJ soils have the supplements of these mobile elements (Ca, Na and K) by soil erosion. As shown in Figure 3, Al_2O_3, retained within clay particles, was depleted reflecting the clay particles loss in the BYSD profile. This result is in agreement with the negative correlation (R^2 = 0.922) between ¹³⁷Cs activities and Al_2O_3/TiO_2 ratios in BYSD profile (Figure 8b). The Al_2O_3/TiO_2 ratios of soil samples in the BYSY and BYSJ profiles are decreasing with depth, this is in agreement with the positive correlations between ¹³⁷Cs activities and Al_2O_3/TiO_2 ratios in the BYSY and BYSJ profiles (R^2 = 0.504 and 0.548, respectively). This result reflects the notion that clay particles from the summit component are transported to the shoulder and toeslope components. It is obvious that the lower three samples (dashed area in Figure 8a and b) in the BYSD profile show that the deposited ¹³⁷Cs is resistant to downward leaching

(Zapata 2002).

The volatile content of a soil sample measured by the loss on ignition (LOI) is considered proportional to the amount of hydrated minerals (mainly clay materials) and organic matter (Ji et al. 2004; Babechuk et al. 2014). As shown (Figure 8c), the relationship between ¹³⁷Cs activities and LOI values are positive and significantly correlated. The highest positive correlation (R^2 = 0.965) between ¹³⁷Cs activities and LOI values in BYSY indicates the effects of the forest belt located at the shoulder component on the soil organic matter. There was no positive correlation between ¹³⁷Cs activities and LOI values in the BYSD profile perhaps due to the loss of clay particles. Figure 8d showed the positive correlations between ¹³⁷Cs activities and FeO contents in all three soil profiles. Considering that the organic matter is the important reductant in soil profile (Ma et al. 2007), the positive correlations between ¹³⁷Cs activities and FeO contents may be closely associated with organic matter.

These results showed that ¹³⁷Cs activity was significantly positive correlated with clay particles and organic matter, and are in agreement with those reported by other researchers (Zapata 2002;
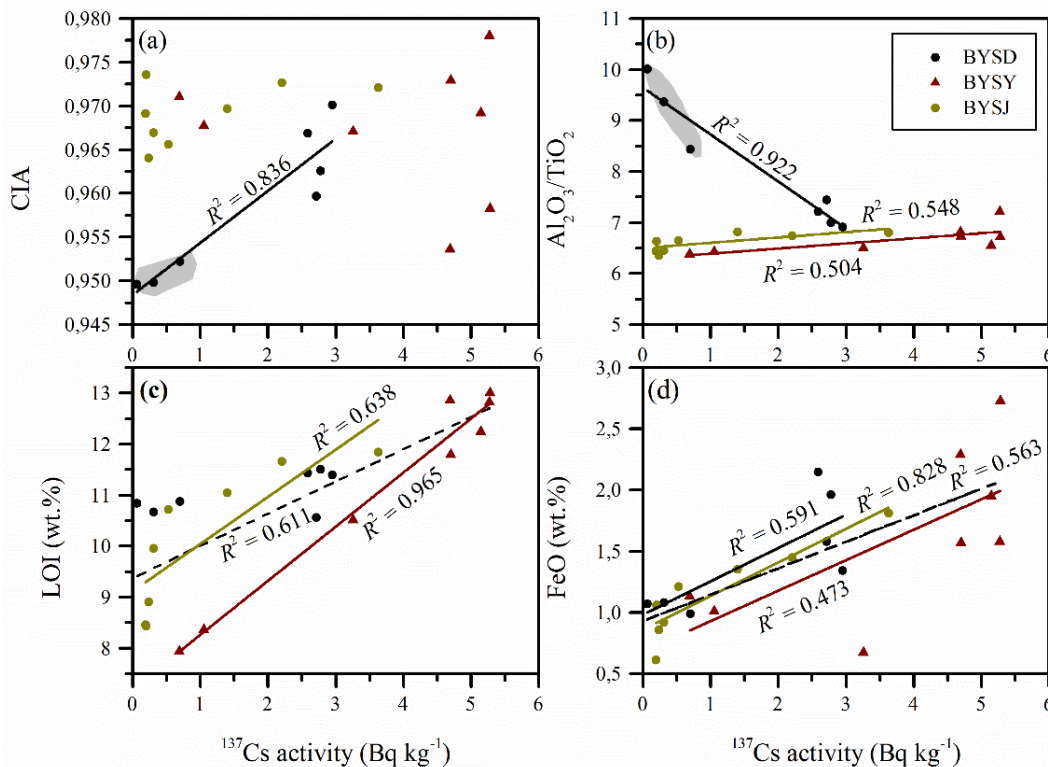
Figure 8 Relationship between ¹³⁷Cs activity (Bq kg⁻¹) and the major element parameters in three soil profiles (BYSD, summit; BYSY, shoulder; BYSJ, toeslope).

Afshar et al. 2010; Rahimi et al. 2013; Gheysari et al. 2016). Furthermore, the pedogenic process and vegatation have an influence on distribution of ^{137}Cs. Overall, it maybe necessary to use ^{137}Cs technique for researching soil erosion along with combination of geochemical methods.

4   Conclusions

The results of this study highlight severe soil erosion (up to 23.30 t ha^{-1} yr^{-1} in the toeslope of the hillslope) in a karst hillslope in Guangxi Province, Southwestern China, using ^{137}Cs radionuclide measurements. The soil redistribution rates were -17.01, 0.40 and -23.30 t ha^{-1} yr^{-1} at the summit, shoulder and toeslope respectively of this studied hillslope. This emphasizes that the effects of human activities, such as the construction of mountain roads and deforestation, can significantly accelerate soil erosion. Therefore, the soil erosion hazard of this study area is high and should not be ignored due to human interference coupled with the low soil formation rate.

Generally, the migration of soil elements was strongly correlated with soil erosion and deposition. These three soil profiles may have been derived from an identical material, and the shoulder and toeslope profiles of this studied hillslope record the inheritance of erosion materials from the summit profile of this hillslope. Relative to the summit of this hillslope, the sesquioxides (Fe_2O_3 and TiO_2) tend to be enriched in the low part (shoulder and toeslope) of this hillslope due to physical migration. The alkalis (CaO, MgO, Na_2O and K_2O) tend to be depleted in the lower part of the hillslope, whereas

P and Si show no obvious trends of enrichment or loss on the hillslope components. In addition, we calculated the depletion and enrichment factors of the three soil profiles (e.g., Ti was used as the immobile element, and the lowermost soil sample in each sample site was selected as the unweathered reference sample). The depletion and enrichment factors of the less mobile elements of Al, Fe and Ti exhibit no obvious changes with depth in the BYSY profile. There are no obvious differences in the depletion and enrichment factors of Fe and Ti and Al and Ti in the BYSD and BYSJ profiles, respectively. In contrast, Al is depleted in the BYSD profile and Fe is enriched in the BYSJ profile, perhaps due to the degradation of organic matter and oxidation-reduction conditions, respectively. The contents of CaO, MgO, K_2O and Na_2O have increased somewhat within the topsoil, perhaps due to human and animal activities.

The results showed that ^{137}Cs activity was significantly positive correlated with clay particles and organic matter, and was affected by the pedogenic process and vegatation. Overall, it maybe necessary to use ^{137}Cs technique for researching soil erosion along with geochemical methods.

References

Afshar FA, Ayoubi S, Jalalian A (2010) Soil redistribution rate and its relationship with soil organic carbon and total nitrogen using ^{137}Cs technique in a cultivated complex hillslope in western Iran. Journal of Environmental Radioactivity 101(8): 606-614.
https://doi.org/10.1016/j.jenvrad.2010.03.008
Arnhold S, Lindner S, Lee B, et al. (2014) Conventional and organic farming: Soil erosion and conservation potential for row crop cultivation. Geoderma 219-220(3): 89-105.
https://doi.org/10.1016/j.geoderma.2013.12.023
Ayoubi S, Khormali F, Sahrawat KL, et al. (2011) Assessing impacts of land use change on soil quality indicators in a loessial soil in Golestan Province, Iran. Journal of Agricultural Science and Technology 13(5): 727-742.
http://oar.icrisat.org/id/eprint/1272

Ayoubi S, Ahmadi M, Abdi MR, et al. (2012a) Relationships of ^{137}Cs inventory with magnetic measures of calcareous soils of hilly region in Iran. Journal of environmental radioactivity 112: 45-51. https://doi.org/10.1016/j.jenvrad.2012.03.012
Ayoubi S, Karchegani PM, Mosaddeghi MR, et al. (2012b) Soil aggregation and organic carbon as affected by topography and land use change in western Iran. Soil and Tillage Research 121: 18-26. https://doi.org/10.1016/j.still.2012.01.011
Ayoubi S, Emami N, Ghaffari N, et al. (2013) Pasture degradation effects on soil quality indicators at different hillslope positions in a semiarid region of western Iran. Environmental Earth Sciences 71(1): 375-381.
https://doi.org/10.1007/s12665-013-2440-x
Babechuk MG, Widdowson M, Kamber BS (2014) Quantifying chemical weathering intensity and trace element release from

two contrasting basalt profiles, Deccan Traps, India. Chemical Geology 363: 56-75. https://doi.org/10.1016/j.chemgeo.2013.10.027

Bai XY (2011) Assessment of sediment and erosion rates by using the caesium-137 technique in a Chinese polygonal karst depression. Environmental Earth Sciences 64(8): 2151-2158. https://doi.org/10.1007/s12665-011-1042-8

Bischoff JL (1969) Red Sea geothermal brine deposits: their mineralogy, chemistry and genesis. In: Degens ET and Ross DA (eds), Hot Brines and Recent Heavy Metal Deposits in the Red Sea. Springer-Verlag, Berlin, Heidelberg, New York. pp 368-401. https://doi.org/10.1007/978-3-662-28603-6

Braun JJ, Ngoupayou JRN, Viers J, et al. (2005) Present weathering rates in a humid tropical watershed: Nsimi, South Cameroon. Geochimica et Cosmochimica Acta 69(2): 357-387. https://doi.org/10.1016/j.gca.2004.06.022

Cao JH, Jiang ZC, Yang DS, et al. (2008) Grading of soil erosion intensity in Southwest karst area of China. Science of Soil and Water Conservation 6(6): 1-7. (In Chinese) https://doi.org/10.3969/j.issn.1672-3007.2008.06.001

Cao JH, Yuan DX, Chris G, et al. (2012) Carbon Fluxes and Sinks: the Consumption of Atmospheric and Soil CO_2 by Carbonate Rock Dissolution. Acta Geologica Sinica 86(4): 963-972. https://doi.org/10.1111/j.1755-6724.2012.00720.x

Collins AL, Walling DE, Sichingabula HM, et al. (2001) Using ^{137}Cs measurements to quantify soil erosion and redistribution rates for areas under different land use in the Upper Kaleya River basin, southern Zambia. Geoderma 104(3-4): 299-323. https://doi.org/10.1016/S0016-7061(01)00087-8

Dai QH, Peng XD, Yang Z, et al. (2017) Runoff and erosion processes on bare slopes in the Karst Rocky Desertification Area. Catena 152: 218-226. https://doi.org/10.1016/j.catena.2017.01.013

Edgington DN, Klump JV, Robbins JA, et al. (1991) Sedimentation rates, residence times and radionuclide inventories in Lake Baikal from ^{137}Cs and ^{210}Pb in sediment cores. Nature 350 (6319): 601-604. https://doi.org/10.1038/350601a0

Feng JL, Zhu LP, Cui ZJ (2009) Quartz features constrain the origin of terra rossa over dolomite on the Yunnan-Guizhou Plateau, China. Journal of Asian Earth Sciences 36(2-3): 156-167. https://doi.org/10.1016/j.jseaes.2009.05.003

Feng T, Chen HS, Zhang W, et al. (2011) ^{137}Cs profile distribution character and its implication for soil erosion on Karst slopes of Northwest Guangxi. Chinese Journal of Applied Ecology 22(3): 593-599. (In Chinese)

Feng T, Chen HG, Polyakov VO, et al. (2016) Soil erosion rates in two karst peak-cluster depression basins of northwest Guangxi, China: Comparison of the RUSLE model with ^{137}Cs measurements. Geomorphology 253: 217-224. https://doi.org/10.1016/j.geomorph.2015.10.013

Fernández C, Vega JA (2016) Evaluation of RUSLE and PESERA models for predicting soil erosion losses in the first year after wildfire in NW Spain. Geoderma 273: 64-72. https://doi.org/10.1016/j.geoderma.2016.03.016

Gheysari F, Ayoubi S, Abdi M (2016) Using Cesium-137 to estimate soil particle redistribution by wind in an arid region of central Iran. Eurasian Journal of Soil Science 5(4): 285-293. http://dx.doi.org/10.18393/ejss.2016.4.285-293

Guo QK, Hao YF, Liu BY (2015) Rates of soil erosion in China: A study based on runoff plot data. Catena 124: 68-76. https://doi.org/10.1016/j.catena.2014.08.013

Hancock G, Wilkinson S, Hawdon A, et al. (2014) Use of fallout tracers [7]Be, ^{210}Pb and ^{137}Cs to distinguish the form of sub-surface soil erosion delivering sediment to rivers in large catchments. Hydrological Processes 28(12): 3855-3874. https://doi.org/10.1002/hyp.9926

Hill IG, Worden RH, Meighan IG (2000) Yttrium: The immobility-mobility transition during basaltic weathering. Geology 28(10): 923-926. https://doi.org/10.1130/0091-7613(2000)28<923:YTITDB>2.0.CO;2

Huang W, Ho HC, Peng YY, et al. (2016) Qualitative risk assessment of soil erosion for karst landforms in Chahe town, Southwest China: A hazard index approach. Catena 144: 184-193. https://doi.org/10.1016/j.catena.2016.05.008

Ji HB, Wang SJ, Ouyang ZY, et al. (2004) Geochemistry of red residua underlying dolomites in karst terrains of Yunnan-Guizhou Plateau: I. The formation of the Pingba profile. Chemical Geology 203(1-2): 1-27. https://doi.org/10.1016/j.chemgeo.2003.08.012

Karchegani PM, Ayoubi S, Mosaddeghi MR, et al. (2012) Soil organic carbon pools in particle-size fractions as affected by slope gradient and land use change in hilly regions, western Iran. Journal of Mountain Science 9(1): 87-95. https://doi.org/10.1007/s11629-012-2211-2

Kheir RB, Abdallah C, Khawlie M (2008) Assessing soil erosion in Mediterranean karst landscapes of Lebanon using remote sensing and GIS. Engineering Geology 99(3-4): 239-254. https://doi.org/10.1016/j.enggeo.2007.11.012

Khormali F, Ajami M, Ayoubi S, et al. (2009) Role of deforestation and hillslope position on soil quality attributes of loess-derived soils in Golestan province, Iran. Agriculture, Ecosystems & Environment 134(3-4): 178-189. https://doi.org/10.1016/j.agee.2009.06.017

Kurtz AZ, Derry LA, Chadwick OA, et al. (2000) Refractory element mobility in volcanic soils. Geology 28(8): 683-686. https://doi.org/10.1130/0091-7613(2000)28<683:REMIVS>2.0.CO;2

Land M, ÖHLANDER B (2000) Chemical weathering rates, erosion rates and mobility of major and trace elements in a Boreal Granitic Till. Aquatic Geochemistry 6(4): 435-460. https://doi.org/10.1023/A:1009644317427

Li H, Zhang XB, Wang KL, et al. (2009) [137]Cs Distribution Characteristics at a Talus-type Karst Slope in Northwestern Guangxi. Journal of Soil and Water Conservation 23(3): 42-47. (In Chinese) https://doi.org/10.3321/j.issn:1009-2242.2009.03.010

Li H, Zhang XB, Wen AB, et al. (2016a) Assessment of Sediment Rate of a Kast Hill Peak-cluster Depression Catchment Using [137]Cs Technique-A Case Study on Yaji Experimental Site. Earth and Environment 44(1): 57-63. (In Chinese) https://doi.org/10.14050/j.cnki.1672-9250.2016.01.008

Li H, Zhang XB, Wang KL, et al. (2010) Assessment of sediment deposition rates in a karst depression of a small catchment in Huanjiang, Guangxi, southwest China, using the cesium-137 technique. Journal of Soil and Water Conservation 65(4): 223-232. https://doi.org/10.2489/jswc.65.4.223

Li Y, Bai XY, Zhou YC, et al. (2016b) Spatial–Temporal Evolution of Soil Erosion in a Typical Mountainous Karst Basin in SW China, Based on GIS and RUSLE. Arabian Journal for Science and Engineering 41(1): 209-221. https://doi.org/10.1007/s13369-015-1742-6

Li YB, Wang SJ, Wei CF, et al. (2006) The spatial distribution of soil loss tolerance in carbonate area in Guizhou province. Earth and Environment 34(4): 36-40. (In Chinese) https://doi.org/10.14050/j.cnki.1672-9250.2006.04.007

Liu CQ (2009) Biogeochemical Processes and Cycling of Nutrients in the Earth's Surface: Cycling of Nutrients in Soil-Plant Systems of Karstic Environments, Southwest China. Science Press, Beijing. pp 123-134. (In Chinese)

Ma JL, Wei GJ, Xu YG, et al. (2007) Mobilization and re-distribution of major and trace elements during extreme weathering of basalt in Hainan Island, South China. Geochimica et Cosmochimica Acta 71(13): 3223-3237. https://doi.org/10.1016/j.gca.2007.03.035

Maynard JB (1992) Chemistry of modern soils as a guide to interpreting Precambrian paleosols. Journal of Geology 100(3): 279-289. https://doi.org/10.1086/629632

Mou BL (1999) Element geochemistry. Peking University Press, Beijing. pp 27-30. (In Chinese)

Muhs DR, Budahn J, Skipp G, et al. (2010) Geochemical and mineralogical evidence for Sahara and Sahel dust additions to Quaternary soils on Lanzarote, eastern Canary Islands, Spain.

Terra Nova 22(6): 399-410.
https://doi.org/10.1111/j.1365-3121.2010.00949.x

Muhs DR, Budahn JR, McGeehin JP, et al. (2013) Loess origin, transport, and deposition over the past 10,000 years, Wrangell-St. Elias National Park, Alaska. Aeolian Research 11(4): 85-99. https://doi.org/10.1016/j.aeolia.2013.06.001

Nesbitt HW, Wilson RE (1992) Recent chemical weathering of basalts. American Journal of science 292 (10): 740-777.
https://doi.org/10.2475/ajs.292.10.740

Nezat CA, Blum JD, Klaue A, et al. (2004) Influence of landscape position and vegetation on long-term weathering rates at the Hubbard Brook Experimental Forest, New Hampshire, USA. Geochimica et Cosmochimica Acta 68(14): 3065-3078. https://doi.org/10.1016/j.gca.2004.01.021

Nosrati K, Haddadchi A, Zare MR, et al. (2015) An evaluation of the role of hillslope components and land use in soil erosion using ^{137}Cs inventory and soil organic carbon stock. Geoderma 243-244: 29-40.
https://doi.org/10.1016/j.geoderma.2014.12.008

Parise M, De WJ, Gutierrez F (2008) Current perspectives on the environmental impacts and hazards in karst. Environmental Geology 58(2): 235-237.
https://doi.org/10.1007/s00254-008-1608-2

Pennock D, Yates T, Braidek J (2007) Soil sampling designs. In: Carter MR and Gregorich EG (Eds), Soil Sampling and Methods of Analysis. Second edition CRC Press, Taylor & Francis Group, Boca Raton. pp 1-14.
https://doi.org/10.1201/9781420005271.ch1

Popa N, Filiche E, Petrovici G, et al. (2011) Using caesium-137 techniques to estimate soil erosion and deposition rates on agricultural fields with specific conservation measures in the Tutova Rolling Hills, Romania. In: IAEA (Ed), Impact of Soil Conservation Measures on Erosion Control and Soil Quality. International Atomic Energy Agency, Vienna, Austria. pp 259-277. http://hdl.handle.net/1969.3/28880

Porto P, Wlling DE, Ferro V (2001) Validating the use of caesium-137 measurements to estimate soil erosion rates in a small drainage basin in Calabria, Southern Italy. Journal of Hydrology 24(1-4): 93-108.
https://doi.org/10.1016/S0022-1694(01)00389-4

Rahimi MR, Ayoubi S, Abdi MR (2013) Magnetic susceptibility and Cs-137 inventory variability as influenced by land use change and slope positions in a hilly, semiarid region of west-central Iran. Journal of Applied Geophysics 89: 68-75.
https://doi.org/10.1016/j.jappgeo.2012.11.009

Rickson RJ (2014) Can control of soil erosion mitigate water pollution by sediments? Science of The Total Environment 468-469: 1187-97.
https://doi.org/10.1016/j.scitotenv.2013.05.057

Riebe CS, Kirchner JW, Granger DE, et al. (2001) Strong tectonic and weak climatic control of long-term chemical weathering rates. Geology 29(6): 511-514.
https://doi.org/10.1130/0091-7613(2001)029<0511:STAWCC>2.0.CO;2

Riebe CS, Kirchner JW, Finkel RC (2003) Long-term rates of chemical weathering and physical erosion from cosmogenic nuclides and geochemical mass balance. Geochimica et Cosmochimica Acta 67(22): 4411-4427.
https://doi.org/10.1016/S0016-7037(03)00382-X

Runge ECA, Walker TW, Howarth DT (1974) A study of late Pleistocene loess deposits, South Canterbury, New Zealand. Part I. Forms and amounts of phosphorus compared with other techniques for identifying paleosols. Quaternary Research 4(1): 76-84.
https://doi.org/10.1016/0033-5894(74)90065-9

Schaller M, Blum JD, Ehlers TA (2009) Combining cosmogenic nuclides and major elements from moraine soil profiles to improve weathering rate estimates. Geomorphology 106(3-4): 198-205. https://doi.org/10.1016/j.geomorph.2008.10.014

Schroth AW, Crusius J, Sholkovitz ER, et al. (2009) Iron solubility driven by speciation in dust sources to the ocean.

Nature Geoscience 2(5): 337-340.
https://doi.org/10.1038/ngeo501

Shi ZL, Wen AB, Zhang XB, et al. (2012) ^{137}Cs and [210]Pb[ex] as soil erosion tracers in the hilly Sichuan Basin and the Three Gorges area of China. Journal of Mountain Science 9(1): 27-33. https://doi.org/10.1007/s11629-012-2200-5

Song ZL, Liu CQ, Han GL, et al. (2006) Enrichment and release of rare earth elements during weathering of sedimentary rocks in Wujiang catchments, Southwest China. Journal of Rare Earths 24 (4): 491-496.
https://doi.org/10.1016/S1002-0721(06)60149-X

Systems Creative Research (2016) The Survey System.
https://www.surveysystem.com/sscalc.htm

Taitel-Goldman N, Koch CB, Singer A (2004) Si-associated goethite in hydrothermal sediments of the Atlantis II and Thetis Deeps, Red Sea. Clays and Clay Minerals 52(1): 115-129.
https://doi.org/10.1346/CCMN.2004.0520111

Taylor A, Blum JD (1995) Relation between soil age and silicate weathering rates determined from the chemical evolution of a glacial chronosequence. Geology 23(11): 979–982.
https://doi.org/10.1130/0091-7613(1995)023<0979:RBSAAS>2.3.CO;2

Taylor SR, McLennan SM (1985) The Continental Crust: its Composition and Evolution. Blackwell Scientific Editor, Oxford. p 312.

Viers J, Dupré B, Braun JJ, et al. (2000) Major and trace element abundances, and strontium isotopes in the Nyong basin rivers (Cameroon): Constraints on chemical weathering processes and elements transport mechanisms in humid tropical environments. Chemcial Geology 169(1-2): 211-241.
https://doi.org/10.1016/S0009-2541(00)00298-9

Walling DE, Quine TA (1990) Calibration of caesium-137 measurements to provide quantitative erosion rate data. Land Degradation & Development 2(3): 161-175.
https://doi.org/10.1002/ldr.3400020302

Walling DE, Quine TA (1993) Use of caesium-137 as a tracer of erosion and sedimentation : handbook for the application of the caesium-137 technique. UK Overseas Development Administration Research Scheme R4579, Department of Geography, University of Exeter, UK. pp 15-97.

Young GM, Nesbitt HW (1998) Processes controlling the distribution of Ti and Al in weathering profiles, siliciclastic sediments and sedimentary rocks. Journal of Sedimentary Research 68(3): 448-455. https://doi.org/10.2110/jsr.68.448

Yousefifard M, Ayoubi S, Jalalian A, et al. (2012) Mass balance of major elements in relation to weathering in soils developed on igneous rocks in a semiarid region, northwestern Iran. Journal of Mountain Science 9(1): 41-58.
https://doi.org/10.1007/s11629-012-2208-x

Zapata F (2002) Handbook for the assessment of soil erosion and sedimentation using environmental radionuclides. Kluwer Academic Publishers, London, Vienna.

Zhang M, Yang H, Xu C, et al. (2009a) Determining soil redistribution in Dian Lake catchment by com- bined use of caesium-137 and selected chemical properties. Ecological Economy 5(1): 91-100.

Zhang XB, Higgitt DI, Walling DE (1990) A preliminary assessment of the potential for using caesium-137 to estimate rates of soil erosion in the Loess Plateau of China. Hydrological Sciences Journal 35(3): 243-252.
https://doi.org/10.1080/02626669009492427

Zhang XB, Bai XY, Li H, et al. (2017) Contrast of ^{137}Cs content in slope soil with depressions, and pond sediments - sediments sources, transportion and balance of karst basin in SW China. Earth and Environment 45(3): 247-258. (In Chinese)
https://doi.org/10.14050/j.cnki.1672-9250.2017.03.001

Zhang Y, Gao X, Zhong ZY, et al. (2009b) Sediment accumulation of Dianchi Lake determined by ^{137}Cs dating. Journal of Geographical Sciences 19(2): 225-238.
https://doi.org/10.1007/s11442-009-0225-7